

Amplification of picosecond pulses in F_2^- : LiF crystals synchronously pumped by picosecond and nanosecond laser pulses

T.T. Basiev, A.Ya. Karasik, V.A. Konyushkin, V.V. Osiko, A.G. Papashvili, D.S. Chunaev

Abstract. A method for amplification of picosecond pulses in F_2^- : LiF crystals synchronously pumped by picosecond and nanosecond pulses is proposed and demonstrated. Due to two-stage amplification of a train of 22-ps, 1150-nm SRS pulses generated by a PbMoO₄ crystal, a power gain of $(2 - 4) \times 10^3$ is achieved and single 6-ps, 0.88-mJ pulses are obtained.

Keywords: F_2^- : LiF crystals, synchronous pumping, picosecond and nanosecond pulses.

The LiF crystals with colour centres have broad (~ 2000 cm⁻¹) absorption and luminescence bands, large cross sections for radiative transitions and high quantum yield of luminescence, which makes them promising for generation of nanosecond, picosecond, and femtosecond light pulses [1–4]. The efficient use of F_2^- : LiF crystals for amplifying nanosecond pulses tunable in the 1090–1270-nm region has been demonstrated in papers [5, 6]. Note that LiF crystals with colour centres are superior in some spectral and optomechanical characteristic [1] to the well-known dye media and ion-doped glasses and crystals applied for amplification of picosecond and femtosecond pulses [7]. In this paper, we studied for the first time the amplification of picosecond pulses in LiF crystals with the F_2^- colour centres synchronously pumped by picosecond and nanosecond laser pulses.

The scheme of the experimental setup is shown in Fig. 1. A passively mode-locked TEM₀₀ Nd³⁺ : YLiF₄ (Nd : YLF) laser with a saturable dye-doped polymer film absorber was used as a master oscillator. The laser emitted ~ 100 -ns trains of ~ 22 -ps, 1047-nm pulses [curve (1) in Fig. 2].

The laser radiation was focused into a 30-mm long nonlinear PbMoO₄ crystal, in which a train of the 20–22-ps SRS pulses was generated at the Stokes wavelength 1150 nm [8]. A F_2^- : LiF crystal placed behind the PbMoO₄ crystal was pumped by the 1047-nm picosecond pulses propagated through the SRS crystal. The maximum of the gain band of F_2^- colour centres is close to the wavelength 1150 nm of the amplified SRS radiation. The focusing of laser radiation

through the nonlinear SRS crystal to F_2^- : LiF amplifier 1 allows us to perform the synchronous amplification of the entire train of picosecond SRS pulses [curve (2) in Fig. 2]. The use of such an amplifier synchronously pumped by picosecond pulses substantially improves the spatial directivity of the SRS beam because amplification is developed only within a narrow pump channel of the F_2^- : LiF amplifier.

After the synchronous amplification of picosecond SRS pulses described above, the energy of the entire SRS train increased by an order of magnitude (from 4.4 to 44 μ J). The energy gain for pulses varied from pulse to pulse within 8–12 due to the amplitude instability caused by spontaneous noise typical for SRS. The duration of the 19–22-ps SRS pulses decreased after such amplification in the F_2^- : LiF crystal down to 7–8 ps, which was accompanied by the corresponding increase in their peak power.

The amplified 7–8-ps, 1150-nm pulses were focused through a dichroic mirror DM3 and a diaphragm to 80-mm long F_2^- : LiF crystal amplifier 2 with Brewster faces. This amplifier provided the amplification of picosecond SRS pulses upon pumping by collinear high-power 1047-nm nanosecond pulses from the Nd : YLF laser reflected from the mirror DM2. The laser resonator was formed by a highly reflecting spherical mirror with the radius of curvature $r = 3$ m and a resonance reflector stack of three glass plates with the reflectivity $R = 30\%$. The resonator also contained a third F_2^- : LiF crystal used for passive Q -switching. To bleach this Q switch for a synchronous triggering of the nanosecond and picosecond lasers, a train of picosecond pulses split from the radiation of the master oscillator by semitransparent dichroic mirrors DM1 and DM2 was directed to the resonator of the nanosecond laser. By varying with the help of the mirror DM2 alignment the energy of the 1047-nm picosecond radiation directed to the resonator of the nanosecond Nd : YLF laser 2 and changing the energy of the flashlamp pump of the laser, we could bleach the nanosecond F_2^- : LiF Q switch synchronously with the selected picosecond pulse in the train.

As a result, Nd : YLF laser 2 emitted high-power 10-ns pulses synchronised with the 7–8-ps SRS pulses. These pulses were focused into crystal amplifier 2 with the help of a spherical mirror and a plane dichroic mirror DM3. Picosecond radiation amplified in two amplifiers pumped by picosecond and nanosecond pulses was directed to a diffraction grating to separate it from the pump radiation and then to a pyroelectric Joule-meter, a germanium avalanche photodiode, and an Imacon-500 streak camera with a time resolution of 1.5 ps for measuring the energy

T.T. Basiev, A.Ya. Karasik, V.A. Konyushkin, V.V. Osiko, A.G. Papashvili, D.S. Chunaev Laser Materials and Technology Research Center, A.M. Prokhorov General Physics Institute, Russian Academy of Sciences, ul. Vavilova 38, 119991 Moscow, Russia; e-mail: karasik@lst.gpi.ru

Received 20 December 2004; revision received 22 February 2005
Kvantovaya Elektronika 35 (4) 344–346 (2005)
Translated by M.N. Sapozhnikov

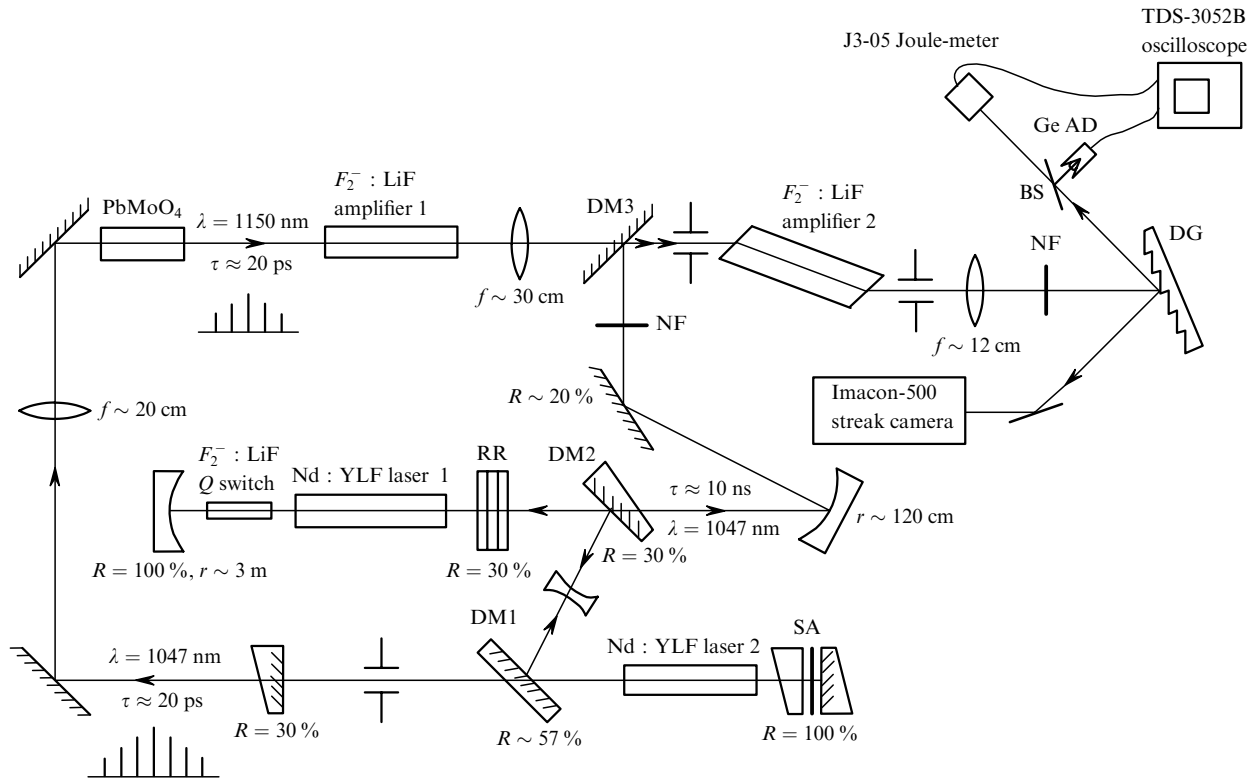


Figure 1. Scheme of the experimental setup: SA: saturable absorber; DM1 and DM2: dichroic mirrors with the reflectivity $R = 57\%$ and 30% , respectively; DM3: dichroic mirror for coupling radiation out the master oscillator; RR: resonance reflector stack with $R = 30\%$; DG: diffraction grating; Ge AP: germanium avalanche photodiode; NF: neutral filters; BS: beamsplitter.

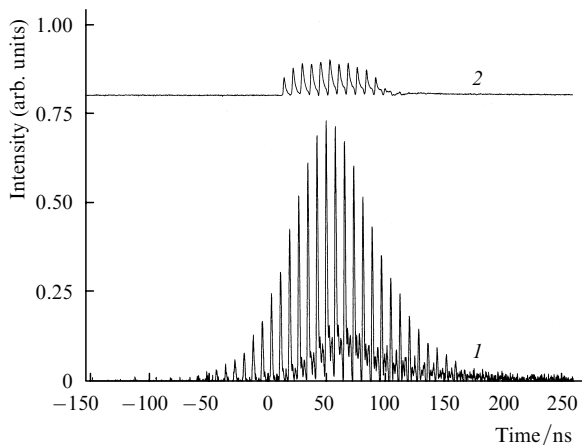


Figure 2. Oscillograms of radiation from the 1047-nm pump Nd:YLF laser (1) and of the amplified train of the 1150-nm SRS pulses in crystal amplifier 1 (2).

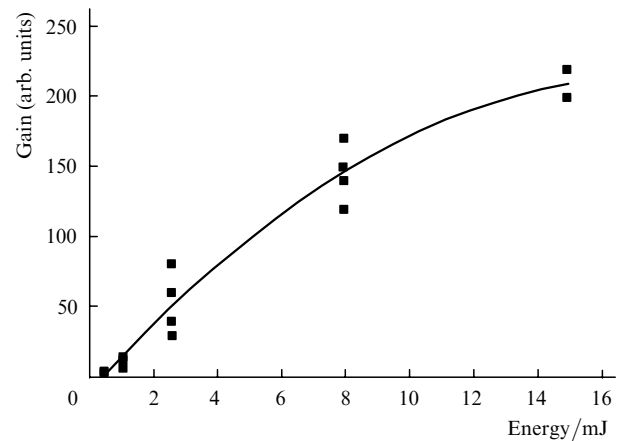


Figure 3. Dependence of the SRS radiation gain on the energy of nanosecond pulses pumping crystal amplifier 2.

and temporal parameters of the amplified radiation.

Figure 3 shows the dependence of the gain of SRS radiation on the energy nanosecond pulses pumping F_2^- :LiF amplifier 2. One can see that the gain curve tends to saturate at the pump energy close to 15 mJ. A comparatively large statistical scatter in the gains upon weak pumping is due to the absence of the accurate locking of the 10-ns pump pulse of the amplifier to a train of picosecond SRS pulses (the jitter was less than 8 ns).

Figure 4 shows the oscillogram of the picosecond 1150-nm radiation after nanosecond crystal amplifier 2. After amplification of the initial train of SRS pulses [curve (2) in

Fig. 2] in the nanosecond amplifier, only one or two high-power pulses dominate in radiation depending on the accuracy of the time synchronisation of picosecond and nanosecond pulses. When only one picosecond pulse is predominantly amplified, the radiation energy measured simultaneously with the oscillogram of the amplified pulse train is only slightly lower than the energy of two high-power pulses (Fig. 4b).

After the two-stage picosecond and nanosecond amplification using 15-mJ nanosecond pumping, the energy of a train of amplified 6-ps pulses was 0.88 mJ, corresponding to the peak pulse power ~ 150 MW. Note that the duration of the compressed amplified pulses was well reproduced.

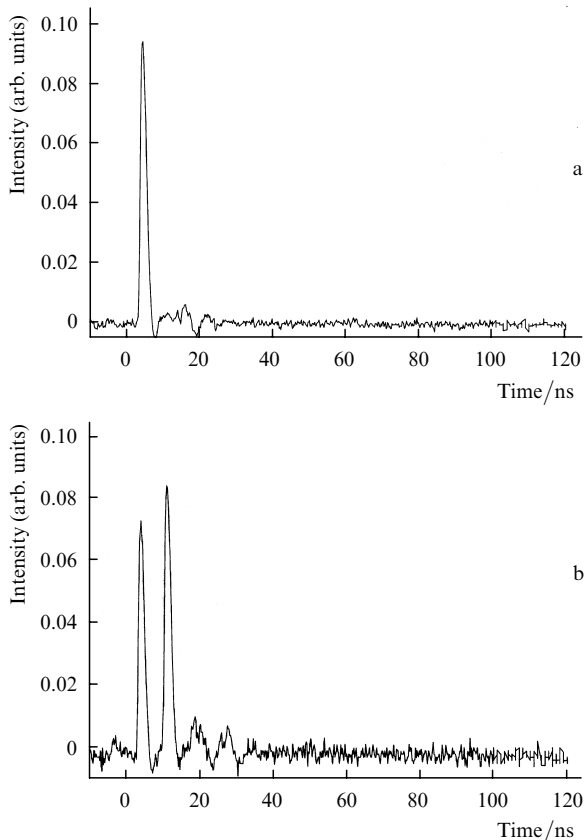


Figure 4. Oscillograms of the 1150-nm picosecond radiation after F_2^- : LiF nanosecond amplifier 2 in the case of amplification of one (a) and two (b) pulses.

The energy was measured with a Joule-meter. The energy gain for a pulse train at the second stage (crystal amplifier 2) was 20. The total two-stage energy gain for the 1150-nm radiation amounted to 200. This value was obtained by dividing the radiation energy at the output of the second amplifier by the energy of the train of SRS pulses at the input of the first amplifier and gives only the lower bound for the pulse energy in the train. Indeed, a train at the input of nanosecond amplifier 2 consists of ~ 10 picosecond pulses separated by the axial interval of ~ 8 ns [curve (2) in Fig. 2], while the output train consists of one–two pulses (Fig. 4). Therefore, the energy gain for one pulse should be multiplied by 4–10 and amounts to $(0.8 - 2) \times 10^3$.

We could also determine independently the synchronous gain of the SRS radiation from the energy after the second stage of the amplifier directly from oscillograms presented in Fig. 4, by normalising the amplitude of the output amplified pulse to the amplitude of the preceding SRS pulses propagated through the amplification stage before the arrival of the nanosecond pump pulse. The gain in the second stage (pumped by nanosecond pulses) measured in this way was between 55 and 80 in different experiments. Taking into account the 8–12-fold amplification in synchronous picosecond amplifier 1, we estimate the total energy gain for a single pulse as $(0.5 - 1) \times 10^3$. Then, taking into account that pulses are shortened approximately by a factor of four during amplification, we obtain the total power gain $\sim (2 - 4) \times 10^3$, in good agreement with the results of measurements described above.

The replacement of the nonlinear PbMoO_4 crystal by a $\text{KGd}(\text{WO}_4)_2$ crystal with the close value of the SRS gain [8] resulted in a change in the temporal parameters of the gain. In the latter crystal, the initially shorter SRS pulses had duration of 8.5 ps, which did not change after the first and second amplification stages. Some reasons for the difference in the transformation of durations of amplified SRS pulses from different crystals were discussed in [8] and require special studies. Note that SRS pulses of duration ~ 1 ps can be generated in oxide nonlinear crystals [8].

Note in conclusion that the picosecond laser emitting ~ 1 -mJ pulses described in this paper is promising for generating terawatt pulses by increasing the number of amplification stages based on the F_2^- : LiF crystals pumped by nanosecond laser pulses.

Acknowledgements. This work was partially supported by the ISTC (Grant No. 2022P) and the Russian Foundation for Basic Research (Grant Nos 04-02-08163ofi_a and 04-02-17004).

References

1. Basiev T.T., Zverev P.G., Mirov S.B. *Handbook of Laser Technology and Applications* (New York: Institute of Physics Publishing, 200) B1.8, p.1.
2. Babushkin A.V., Basiev T.T., Vorob'ev N.S., Mirov S.B., Prokhorov A.M., Serdyuchenko Yu.N., Shchelev M.Ya. *Kvantovaya Elektron.*, **13**, 2262 (1986) [*Sov. J. Quantum Electron.*, **16**, 1492 (1986)].
3. Basiev T.T., Karasik A.Ya., Dergachev A.Yu., Fedorov V.V., Shubichkin R.L. *Kvantovaya Elektron.*, **23**, 1072 (1996) [*Quantum Electron.*, **26**, 1042 (1996)].
4. Zverev P.G., Basiev T.T., Laubereau A. *Novel Lasers and Applications Basic Aspects* (Washington, DC, OSA, 1999) p.57.5.
5. Basiev T.T., Ermakov I.V., Konyushkin V.A., Pukhov K.K., Glasbik M. *Kvantovaya Elektron.*, **25**, 187 (1998) [*Quantum Electron.*, **28**, 179 (1998)]; Basiev T.T., Ermakov I.V., Konyushkin V.A., Pukhov K.K. *Kvantovaya Elektron.*, **31**, 424 (2001) [*Quantum Electron.*, **31**, 424 (2001)].
6. Basiev T.T., Doroshenko M.E., Zverev P.G., Skorniyakov V.V. *Tech. Dig. Conf. on Advanced Solid-State Lasers* (Washington, DC, OSA, 2001) p.54.
7. *Tech. Dig. Conf. on Lasers, Applications, and Technologies* (Moscow: URSS Publishers, 2002).
8. Basiev T.T., Zverev P.G., Karasik A.Ya., Osiko V.V., Sobol' A.A., Chunaev D.S. *Zh. Eksp. Teor. Fiz.*, **126**, 1073 (2004) [*JETP*, **99**, 934 (2004)].